THE BELL SYSTEM TECHNICAL JOURNAL
Vol. 51, No. 9, November, 1972
Printed in U.S.A.

Earthquake Environment for Physical Design: A Statistical Analysis

By S. C. LIU and L. W. FAGEL

(Manuscript received April 14, 1972)

A statistical analysis of nationwide seismic activities is made to determine the level and characteristics of earthquake motions to be expected in different geographical locations. Such information is needed to identify the severity of the earthquake threat to telephone facilities and to specify adequate design requirements. This paper describes the essential seismic environment including the expected earthquake-magnitude levels and the corresponding frequency of occurrence for different seismic-risk zones, and the free-field and in-building motions that might be induced by earthquakes. Stochastic models are used to analyze the earthquake-occurrence statistics, and to describe the induced random ground motions. Historical earthquake data are used to verify the theory and to generate information useful for seismic design.

I. INTRODUCTION

Telephone communications are so vitally important to public health and safety that special efforts must be made to prevent disruption of these services by a destructive earthquake.[1] For this reason, and in order to protect extremely expensive telephone plant investments, it is important to incorporate earthquake-resistant design into telephone facilities. The urgency of safeguarding communications systems against earthquake hazards has become even more evident as a result of experience gained from the recent San Fernando earthquake.[2] At present, earthquake design loads for telephone plants are estimated through use of structural design procedures such as those outlined in the Uniform Building Code (UBC).[3] These procedures may be generally satisfactory for building design, but are not appropriate for determining seismic loads for equipment housed in central office buildings.[4] Consequently, earthquake-resistant guidelines should be established for the physical design of communications facilities, and these guidelines should be

based on realistic estimates of the seismic environments to which telephone plants may be exposed. These environments and the necessary theoretical background for defining them are presented in this paper. The dynamic behavior of telephone structures in these environments and design criteria are not considered.

A statistical study approach is adopted here and historical earthquake data[5] are used both to verify the theoretical analysis and to identify the earthquake environments of engineering significance. The objective in Section II is to derive two types of statistics: macrophenomena, which deal with the single highest value of random parameters that characterize the earthquake occurrence; and microphenomena, which describe the local earthquake motion. In other words, it is a study of the statistical distribution of the magnitude (or intensity) of the largest earthquake in a given area, as well as the distribution of the largest amplitude of the nonstationary, earthquake-induced ground motion. In Section III, the theory is then applied to analyze available earthquake data and to generate information that is important from the viewpoint of seismic design. Geographic regions in this country that have had moderate-to-high levels of seismicity are selected (Fig. 1),[6] and the distribution of the intensity of the maximum annual earthquake for each region is then computed. Earthquake accelerograms along with the expected response spectra for given magnitude levels are presented which can be used for dynamic response analyses of structures.

II. STATISTICAL ANALYSIS OF EARTHQUAKES

Statistical techniques have been applied to many aspects of seismology and earthquake engineering; for example, in the data processing that involves estimating the travel time of seismic waves and locating their origin (epicenter), or in the analysis of seismic actions from a given area. In this section, emphasis is on this latter aspect, i.e., the statistical analysis of seismic action in a certain area from both the global and local standpoints. These two are distinguished by comparing the time scales they involve. The global (or macro-) analysis deals with the earthquake occurrence over a long period of time measured in a multiple of years. In this case, the earthquake-occurrence times and magnitudes (energies) are treated as random sequences. The local (or micro-) analysis deals with the free-field seismic wave motion itself, which generally lasts less than a minute. For each particular event, the local ground motion varies randomly with respect to time and constitutes a stochastic process. The objective of this section is to develop stochastic

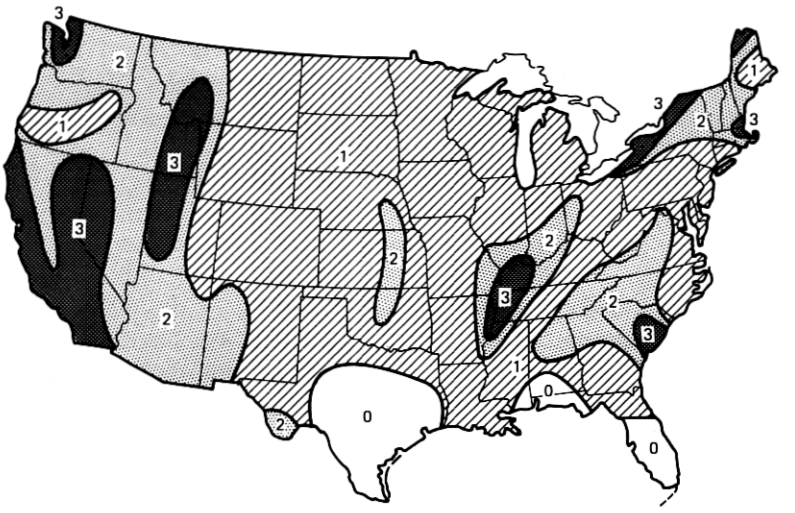

Fig. 1—Earthquake risk map by the National Oceanic and Atmospheric Administration[6] and UBC.[3]

models that are suitable for seismic-risk study, use them to interpret existing earthquake data, and extract information that can be used to establish loading environments for telephone structures located anywhere in the United States.

2.1 *Stochastic Model for Earthquake Occurrence*

Earthquakes can be considered to be a series of events randomly distributed on a real line (representing time), and the sequence of original times $\{t_n\}$ forms a point process.[7] It is further assumed that the joint statistics of the respective number of shocks in any set of intervals are invariant under a translation of these intervals; this implies that $\{t_n\}$ is a stationary point process. The stationary point process generalizes certain aspects of renewal processes; in particular,

the interval lengths $\tau_k = t_k - t_{k-1}$ between successive events need not be independently or identically distributed.

The simplest stationary point process is the Poisson process. Intuitively, the process $\{t_n\}$ can be approximated as a Poisson process if it represents rare events.* More rigorously it requires that τ_k be independently and identically distributed and follow a negative exponential function. Because of the simplicity and fairly general assumptions of the Poisson process, many studies have been made to test its fitness to the earthquake sequences.[9-16] Unfortunately, results of these tests in most cases indicate that the Poisson process is inadequate to explain the time distribution of low-magnitude shocks. The main deficiency of the simple Poisson model is its inability to describe the aftershocks which are often triggered by a large main shock. To account for the occurrence of aftershocks, the simple Poisson model for the main events is generalized to allow for the occurrence of more than one shock in a time unit, and a rate function $g(t)$ defined for $t \geqq 0$ and normalized to unit area is introduced into the generalized model to describe the distribution of the total number of aftershocks.[9] The function $g(t)$ can be either a decaying exponential or an inverse-power relation depending on the magnitude, depth, and location of the main event.[8,16] This model is known as the trigger or cluster model for earthquake processes.

However, for most practical engineering purposes, the simple Poisson model for earthquakes appears to be adequate. In practice, an engineer is concerned with the earthquake risk of structures located in some specific geographic areas. The risk depends heavily on the statistics of large earthquakes of these areas, and the omission of small earthquakes or aftershock processes is relatively unimportant in terms of earthquake risk. For this reason, the simple Poisson process[17] combined with the extreme-value theory[18] is used in this study to derive the distribution function of the magnitude (or intensity, peak ground accleration, etc.) of the largest shock in a time interval.

Let $N(m)$, the expected number of earthquakes in an area per unit time whose magnitude M exceeds m, be given by Gutenberg and Richter's familiar equation[19]

$$\log_{10} N(m) = \mathrm{a} - \mathrm{b}\, m, \qquad m > 0 \tag{1}$$

or, equivalently,

$$N(m) = \alpha e^{-\beta m} \tag{2}$$

* Rare events may be justifiable if we consider only deep earthquakes or very large earthquakes.[8]

where $\alpha = \exp(a \ln 10)$, $\beta = b \ln 10$, and a and b are constants. Then

$$P'(m) = \text{prob}\,(M > m) = \frac{N(m)}{N(0)} = e^{-\beta m} \tag{3}$$

and

$$P(m) = \text{prob}\,(M \leqq m) = 1 - e^{-\beta m}, \qquad m > 0. \tag{4}$$

Therefore, the probability density function of the earthquake magnitude is given by

$$p(m) = dP(m)/dm = \beta e^{-\beta m}, \qquad m > 0 \tag{5}$$

which indicates that the magnitudes of earthquakes are independently and negative-exponentially distributed with a parameter β. From eq. (5), the mean magnitude of all earthquakes of magnitude $m > 0$ and its variance are, respectively, $1/\beta$ and $1/\beta^2$. The mean return period, i.e., the mean interval in years between earthquakes having magnitude $M > m$, is

$$T_m = \frac{1}{N(m)} = (e^{\beta m})/\alpha. \tag{6}$$

From eq. (4) and under the assumption that the number of earth-earthquakes in an interval t follows a Poisson distribution

$$p(n, t) = (\lambda t)^n \exp(-\lambda t)/n!$$

with an average rate $\lambda > 0$ (note that $\alpha = \lambda t$), it can be shown that the magnitude of the largest shock, denoted by y, in the interval has the distribution

$$F(y, t) = \text{prob}\,(\max m \leqq y) = \sum_{n=0}^{\infty} p(n, t)P(y)^n$$

$$= \exp\{-\lambda t[1 - (1 - e^{-\beta y})]\} = \exp(-\lambda t e^{-\beta y}), \qquad y > 0 \tag{7}$$

which is called the distribution of largest values of the first kind. From eq. (7), the probability density function of y in t years becomes:

$$f(y, t) = dF(y, t)/dy = \lambda t \beta \exp(-\beta y - \lambda t e^{-\beta y}), \qquad y > 0. \tag{8}$$

A concise yet detailed analysis of the above extreme value model and its application in earthquake statistics has been given by Epstein and Lomnitz.[17] It is noted that the most significant parameters in the postulated earthquake occurrence model are λ and β. Based on historical earthquake magnitude data, the values of λ and β can be estimated by

a least-squares regression procedure or by using Gumbel's extreme-value plot, on which $F(y, t)$ should asymptotically fit a straight line. This latter approach is used in Section III to analyze data from various active seismic regions in the country.

2.2 *Stochastic Model for Earthquake Ground Motion*

Attention is now directed to the microanalysis of earthquake statistics; a description of a stochastic model which can be used for this analysis follows. The objective is to derive the probability distribution function of the single highest amplitude of the earthquake ground motion having a given magnitude, as well as statistics of its induced structural response.

2.2.1 *Multiplicative Process Model*

Various stationary and nonstationary models have been proposed to describe the earthquake ground motion.[20] The approach is to adopt here the multiplicative process representative for the ground acceleration $x(t)$ given by

$$x(t) = \phi(t)n(t), \tag{9}$$

where $\phi(t)$ is a deterministic envelope function and $n(t)$ is a Gaussian stationary process with power spectral density $S_n(\omega)$ and autocorrelation function $R_n(\tau)$. The following expression taken from Jennings, et al.[21] represents the envelope function (see Fig. 2):

$$\phi(t) = \begin{cases} (t/t_1)^2 & 0 \leqq t \leqq t_1 , \\ 1 & t_1 \leqq t \leqq t_2 , \\ e^{-\mu(t-t_2)} & t_2 \leqq t \leqq t_3 , \end{cases} \tag{10}$$

where $\mu > 0$ is a constant and t_3 is the total duration of the accelerogram.

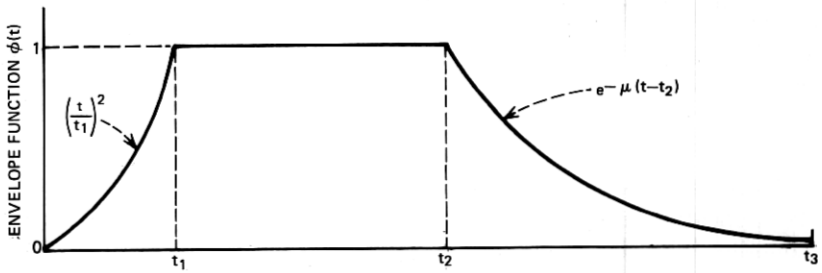

Fig. 2—Envelope function for earthquake accelerogram.

Under the assumption that the process $n(t)$ is the response of a linear ground filter with characteristic constants ω_g (representing natural frequency) and ξ_g (representing damping) to a Gaussian white noise with uniform power spectral density S, it can be shown[22] that the expected number of overshoots of $x(t)$ per unit time over the double barrier $x = \pm a$ is

$$m_{|a|}(t) = \frac{1}{\pi\sigma_n\phi^2} \exp\left(-\frac{a^2}{2\sigma_n^2\phi^2}\right)\left[\sigma_{\dot{n}}\phi^2 \exp\left(-\frac{a^2\dot{\phi}^2}{2\sigma_{\dot{n}}^2\phi^4}\right) + \frac{\pi}{2} a\dot{\phi} \operatorname{erfc}\left(\frac{a\dot{\phi}}{\sqrt{2}\,\sigma_{\dot{n}}\phi}\right)\right], \qquad (11)$$

where σ_n and $\sigma_{\dot{n}}$ are standard deviations of $n(t)$ and $\dot{n}(t) = dn/dt$, respectively.

It is also possible to derive the distribution $F(z, t)$ of z, the largest value of $x(t)$ in a duration t, by again assuming that the probability distribution for n crossings in t is Poisson with a nonhomogeneous rate $N_{|a|}(t) = \int_0^t m_{|a|}(\tau)\, d\tau$. By this assumption, which is good for high crossing levels, it can be easily found that $F(z, t) = \exp[-N_{|z|}(t)]$ and the density function is $f(z, t) = dF/dt$. It should be noted that the analytical solution to the probability density function $f(z, t)$ is extremely complex even when $\phi(t)$ has a very simple expression. However, the mean and mean-square values of z in an interval t and its variance can be evaluated numerically without much difficulty. Note that these quantities are time-dependent and are functions of S, the spectral density of the white noise that produces $n(t)$. Some useful approximate solutions of the above statistical quantities are given in Appendix A.

2.3 *Distribution of the Maximum Structural Response*

The effect of the above earthquake process on structures can be represented by its response spectra, the maximum responses of single-degree-of-freedom systems with natural frequency ω_o and damping ξ_o. The primary interest is to find the expected response spectra and the associated variances. Since the input process $x(t)$ is nonstationary, the response process $u(t)$ is also nonstationary. The exact statistical behavior of $u(t)$ is, therefore, very difficult to obtain. However, results of practical value can reasonably be obtained by considering either a stationary approximation or a Monte Carlo approach. The latter is more accurate, of course, and is used in this study; however, the stationary approximation method is sometimes preferred because it can provide quicker and less-expensive numerical results.

2.3.1 *Stationary Approximation*

This method provides the approximation of the expected response spectrum to an input earthquake process and follows directly from the same approximate treatment as that used in arriving at eqs. (13) to (17) of Appendix A. Here it is assumed that the initial build-up and final decaying portions of $x(t)$ do not significantly affect the structural response $u(t)$, and therefore, $u(t)$ can also be treated as stationary. On this basis, eqs. (13) to (17) will also be valid to approximate the corresponding quantities for the response process after replacing z by $\max \mid u \mid$, σ_n by σ_u, which is the standard deviation of $u(t)$, and ν_n by $\nu_u = \sigma_{\dot{u}}/(\pi\sigma_u)$ = the zero crossing rate of $u(t)$ from both above and below. The values of σ_u and $\sigma_{\dot{u}}$ (the standard deviation of $\dot{u}(t) = du/dt$) can be easily determined by integrating the power spectral density functions $S_u(\omega)$ and $S_{\dot{u}}(\omega) = \omega^2 S_u(\omega)$ respectively. The function $S_u(\omega)$ is given by $S_n(\omega) \mid H_s(\omega) \mid^2$, where $H_s(\omega) = (\omega_o^2 - \omega^2 + 2i\xi_o\omega_o\omega)^{-1}$ is the transfer function of the structure and based on the ground motion model, $S_n(\omega) = S/[(\omega^2 - \omega_g^2)^2 + 4\xi_g^2\omega^2\omega_g^2]$. The results for the statistics of $u(t)$ in terms of given input and system parameters are given in Appendix B.

2.3.2 *Monte Carlo Computation*

The second approach to establish the distribution of the maximum structure response is Monte Carlo computation; the procedure is demonstrated below. For each magnitude level M, the expected spectral intensity $SI_{0.2} = \int_{0.1}^{2.5} S_v(T_o, 0.2)\, dT_o$, representing the damage (response) potential of an earthquake,[23] is obtained from Fig. 3, in which 0.2 is the associated damping ratio, $T_o = 2\pi/\omega_o$ = the natural period

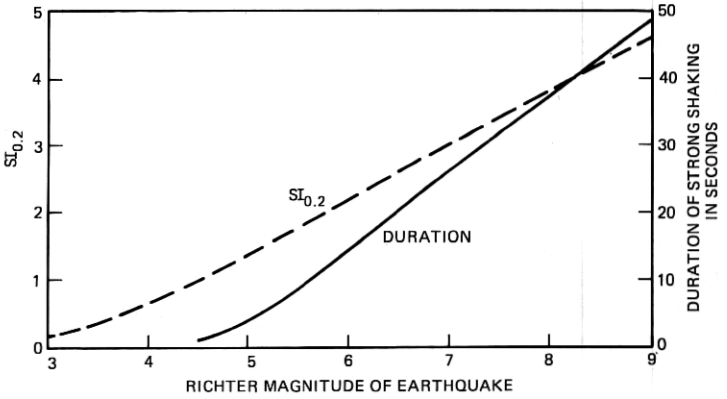

Fig. 3—$SI_{0.2}$ Intensity and duration of strong shaking versus Richter magnitude.

of the structure, and the duration of the strong shocking t_0 is also given in this figure. The desired earthquake process $x(t)$ is obtained by first generating the stationary process $n(t)$ on a computer by the standard method,[24] then shaping $n(t)$ by $\phi(t)$, and then normalizing it to match the expected spectral intensity $SI_{0.2}$. The response spectra $S_v(\omega_o, \xi_o)$ of each of the sample functions of $x(t)$ are then computed and averaged to obtain $E[S_v]$, where E denotes the ensemble average, and σ_{S_v}, the corresponding standard deviation. By this procedure the numerical solutions converge to the true ones rapidly as the sample size increases. With efficient algorithms and computer facilities available, this method should prove satisfactory for practical purposes. This method is used in the next section to generate the desirable ensemble of earthquake accelerograms and the associated response spectra.

III. APPLICATIONS

The statistics of earthquakes that can occur within various specified geographic regions in the United States are next estimated using historical data and the theories given in the previous section.

3.1 *Return Periods of Earthquakes*

The distribution of the magnitude of the largest annual earthquakes that occur within a particular region is given by eq. (7) with $t = 1$ year. Gumbel's probability paper[18] for extreme-value distributions of the first kind is used to plot this data. If the variate m does indeed follow a Poisson distribution, the distribution $F(y, t)$ in eq. (7) will plot in Gumbel's paper as a straight line. Earthquake return periods are equal to $(1 - F(y, t))^{-1}$; therefore, the required information is automatically generated when the Gumbel probability paper is used.

The procedure for constructing an extreme-value plot for a specified region is as follows. The highest annual modified Mercalli Intensity (I) [y in eq. (7)] for n years, as given in the U. S. earthquake catalogue,[5] are tabulated in order of increasing size: $y(1) \leqq y(2) \leqq \cdots \leqq y(n)$. For each $y(i)$, the associated value of $F(y(i), 1) = i/(n + 1)$. The computed $F(y(i), 1)$'s are plotted on an extreme-value graph versus Richter Magnitude (M) by using the relationship $M = 1 + 2I/3$ as proposed by Gutenberg and Richter.[19]

The geographic regions that have been referred to are selected after first dividing a map of the United States into 1-degree-longitude by 1-degree-latitude rectangular areas (each segment is approximately 50 by 70 miles) in Fig. 4. Each rectangle contains two numbers that are

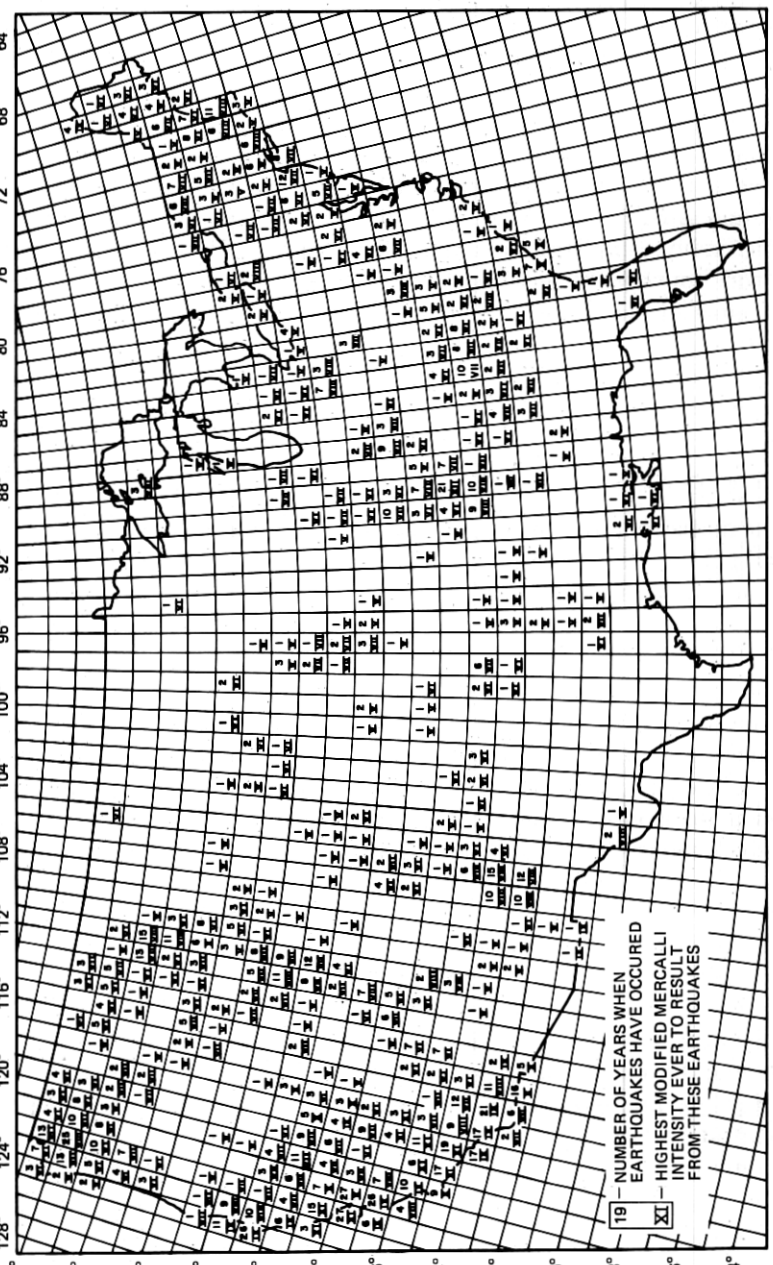

Fig. 4—Earthquake intensity data map of the United States.

obtained from historical data[5] if an earthquake of Modified Mercalli Intensity (I) greater than V had ever occurred within its boundaries. The arabic number represents the number of years when earthquakes have occurred, and the Roman numeral represents the largest intensity associated with any of those events. This information complements the seismic risk map in Fig. 1, and the two are considered together for defining boundaries around areas that appear to have comparable seismic history. These areas and boundaries are shown in Fig. 5a, and graphs showing Richter magnitude versus estimated return periods for earthquakes that may occur within these boundaries are shown in Fig. 5b. The largest magnitude distributions are plotted in Gumbel's paper as straight lines in Fig. 5b with its slope being proportional to the standard deviation of the maximum magnitude levels. Note that these distributions are based on all earthquakes that occurred in the identified areas with the exception of the 1811–1812 New Madrid, Mo. and the 1886 Charleston, South Carolina earthquakes. The return periods for these two violent events are estimated to be thousands of years; consequently, these are not regarded as meaningful data. Notice also that areas A, E, and H (see Fig. 5a), although geographically discontinuous, have very similar and comparable seismicity (Fig. 4) and the calculated distribution data for these areas are represented by a common straight line in the Gumbel's probability paper (Fig. 5b). Although various methods can be used to estimate the parameters of extreme distributions with different degrees of significance, such efforts are not warranted because a slight variation in the estimation is not an overriding concern in engineering risk analysis. Based on the same reason, distributions for areas B, F, G, I, J are also approximated by a common straight line.

Based on the results of Fig. 5b, maps such as that in Fig. 6 showing the Richter magnitude levels associated with different return periods can be constructed. Such maps are of value because they not only show the different degree of severity of earthquake threat in various regions, but also give the information as to how frequently the damaging earthquakes would be expected to occur in these regions. It may be noted that similarities exist between Figs. 1 and 6 because the seismic-risk map was referenced in selecting the boundaries in the return-period study. Some of the dissimilarities are noteworthy, however:

(*i*) The boundaries of the zone-3 area in parts of California and Nevada are not the same as those around the high-Richter-magnitude area in these states. The Great Central Valley below the 40th parallel has had greater seismic activity than most

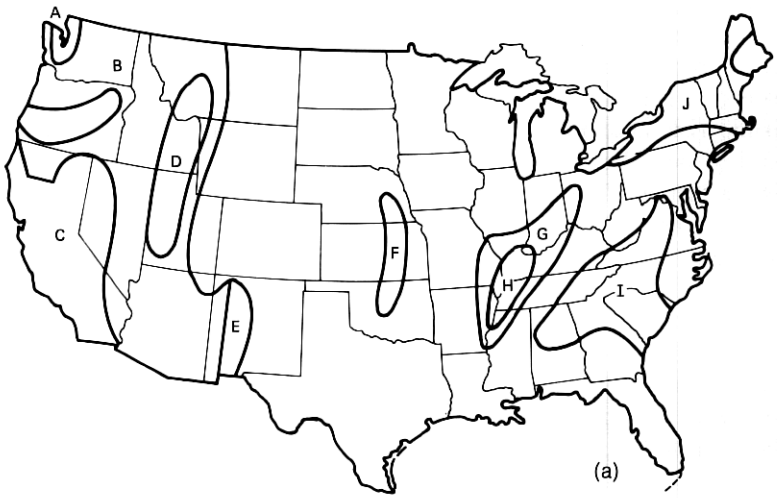

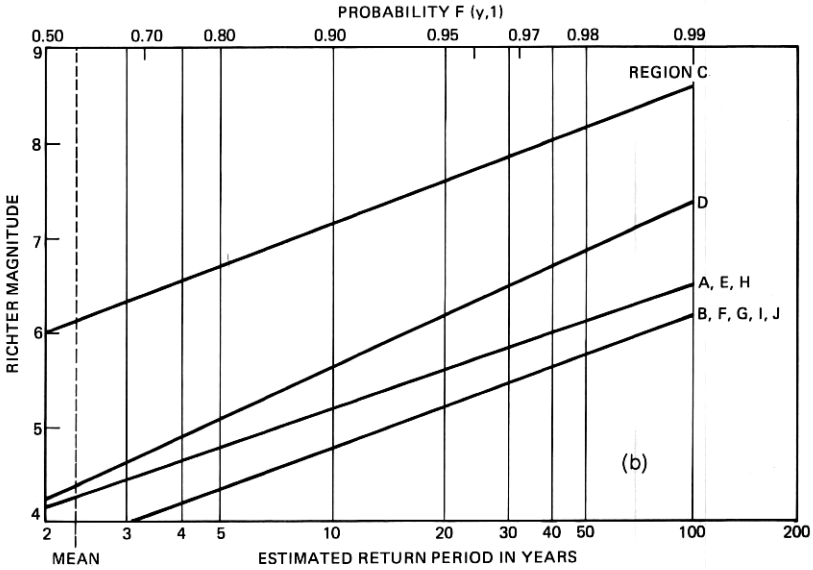

Fig. 5a—Seismic regions and boundaries for magnitude distribution analysis.
Fig. 5b—Earthquake Richter magnitude versus estimated return period.

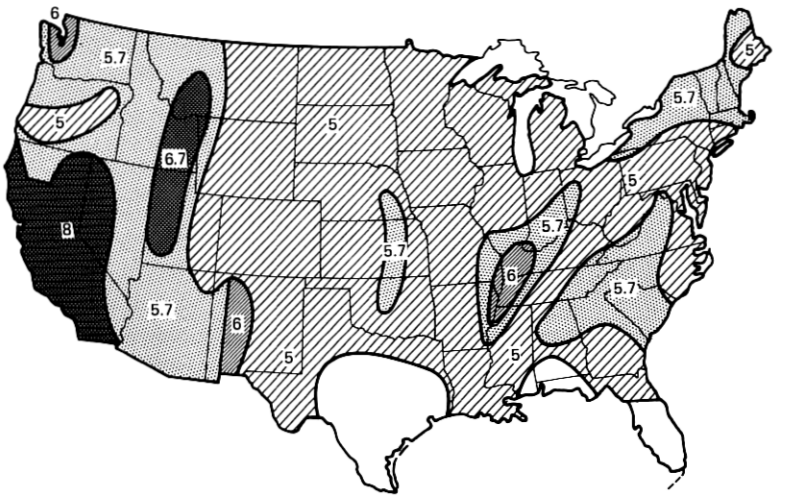

Fig. 6—Estimated maximum earthquake magnitudes for 40-year return period.

other western states, zone-2 areas; therefore, its data is considered with that of the neighboring zone-3 area.

(*ii*) California and Nevada have earthquake histories that indicate that larger earthquakes will occur in this area than in other zone-3 areas for the same return periods. The estimated maximum Richter magnitude is 8, whereas it is 6 for the Seattle area, 6.7 for the Montana-Iowa-Utah zone-3 area, 6 for the St. Louis area, and 5.7 for the Boston and Charleston, S. C. areas. Boston and Charleston do not appear to be more earthquake-prone than their respective surroundings which is in constrast to the information in Fig. 1.

(*iii*) Western New Mexico appears to have more earthquake potential than the rest of the Western United States, zone-2 region.

(*iv*) A small area within the western part of Texas is designated as zone 2 solely because of the $M = 6.4$, 8/13/31 earthquake at Mt. Livermore. Insufficient data prevents an extreme value distribution to be established; therefore, the region is not designated to be different in Fig. 6 from its surroundings.

Ground shaking that may occur in territories that are designated by an $M = 5$ design level in Fig. 6 (zone-1 in Fig. 1) are generally expected to be too small to be of engineering-design interest. Ground motion in

these areas could result from small-magnitude, local tremors or large-magnitude distant earthquakes; however, it does not appear to be a significant threat. The $M = 5$ design level shown for these areas in Fig. 6 should be regarded as an upper bound that is not necessarily applicable, particularly in geographic areas that have never experienced earthquakes (see Fig. 4).

3.2 *Free-Field Ground Motions*

It has not been feasible for building engineers or seismologists to consider geological conditions and then make precise, a priori predictions of ground motions that will occur at any particular point on the earth's surface during an earthquake. This is so because most dependent parameters such as earthquake magnitude, focal depth, epicentral distance, slipped fault length, propagation path, and soil-media properties, are usually not adequately known.

A more direct and realistic approach to defining ground motions is to artificially synthesize them using characteristic parameters from past earthquake accelerogram measurements, such as dominant frequency, amplitude (Fig. 7), spectrum intensity, and duration of ground motion (Fig. 3), etc. Dominant frequencies of an earthquake are defined here as those corresponding to the dominant peak in the Fourier spectrum of the accelerogram. These are known to range between 6 and 60 radians/s with a mean value of approximately 15 radians/s (Fig. 8). Peak acceleration amplitudes can be generally related to magnitude by the curve in Fig. 7. These are upper-bound values for compact alluvium. Accelerations on sites of different geology would fluctuate about the values shown in Fig. 7.

The procedure and references for synthesizing an artificial earthquake

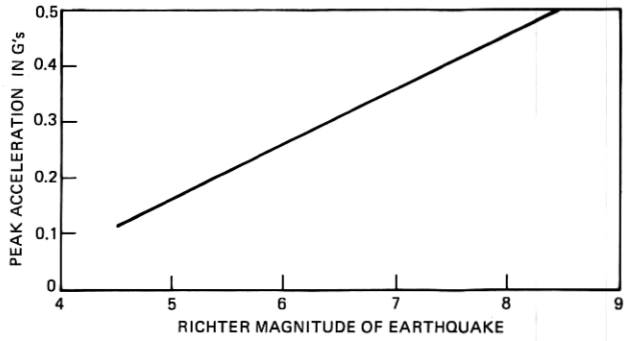

Fig. 7—Expected peak amplitudes of earthquake accelerograms.

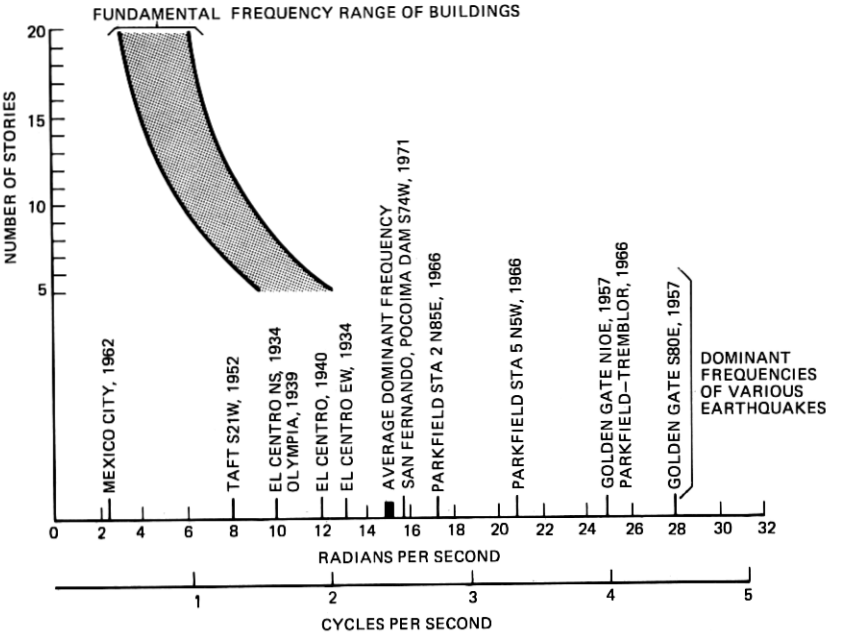

Fig. 8—Typical fundamental frequencies of multistory buildings and dominant frequencies of strong-motion earthquakes.

using the above parameters and a digital computer are given in Refs. 20 and 23. A sample accelerogram for an earthquake of Richter magnitude 6.3 is shown in Fig. 9a. The assumed values of the dependent parameters used to create this waveform are a dominant frequency of 15 radians/s, an $SI_{0.2}$ of 2.3, and an envelope function which is comprised of a 3-second buildup, 9 seconds of strong stationary shaking, and an exponential decay that lasts for 18 seconds. The waveform in Fig. 9a is one of an ensemble of 25 synthetic earthquakes generated according to the Monte Carlo method described earlier, and it corresponds to the average of the peak accelerations from the ensemble. This is 0.28 g's which coincides with the acceleration value given by both Housner[23] and Gutenberg-Richter[19] for an earthquake of this magnitude. The velocity and displacement functions corresponding to this particular accelerogram, obtained by integrations after performing baseline corrections, are shown in Figs. 9b and 9c. The peak amplitudes are 1.5 ft/s and 1.3 ft respectively.

Artificial earthquakes corresponding to different Richter magnitudes and dominant frequencies can be synthesized in the same manner. If the

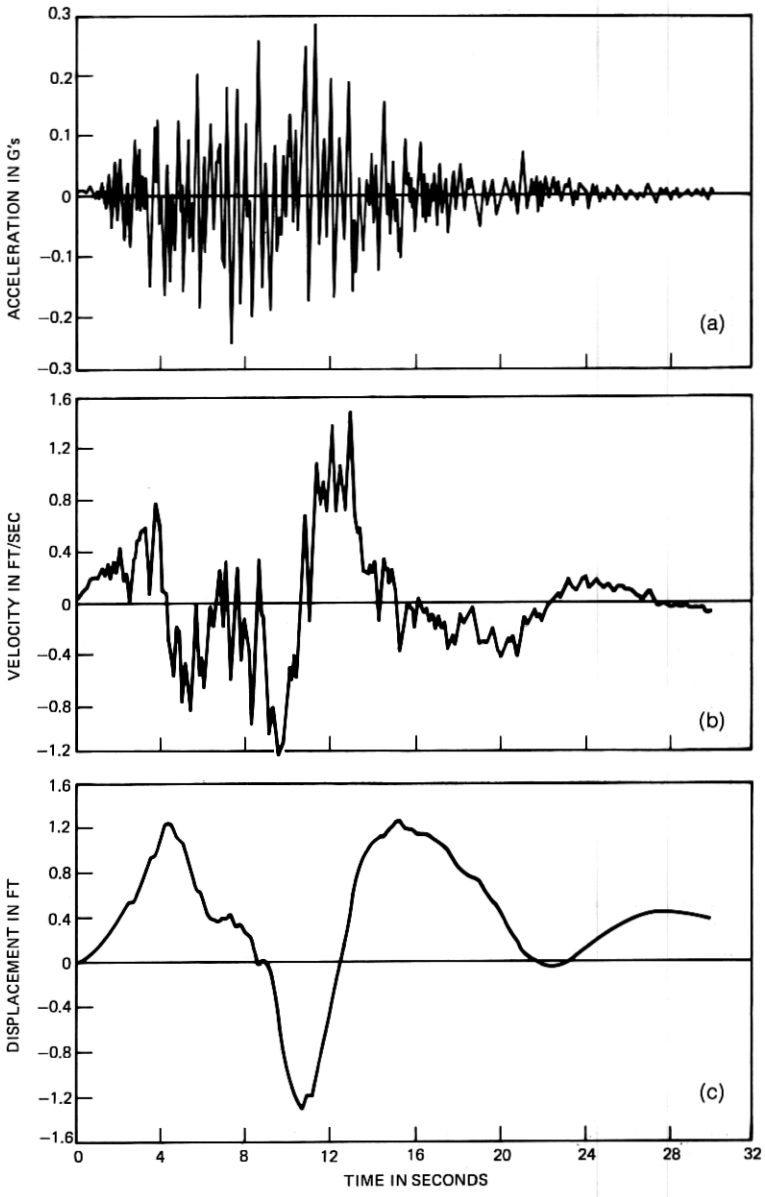

Fig. 9—Acceleration, velocity, and displacement time-histories of synthetic earthquake with $M = 6.3$.

dominant frequency is close to the average (15 radians/s), it is simpler to approximate other horizontal ground motions by scaling the previously mentioned waveforms with the factors shown in Table I which are the $SI_{0.2}$ values normalized to 1.0 for a magnitude 6.3 earthquake. This procedure will yield peak accelerations for different magnitudes of earthquakes that are approximately in agreement with Housner's data[23] (Fig. 7).

Figures 10a, 10b, and 10c are acceleration, velocity, and displacement response spectra of the accelerogram shown in Fig. 9a for damping ratios of 2 percent, 5 percent, and 10 percent. It is apparent that the acceleration, velocity, and displacement time functions of Figs. 9a, b and c together with these response spectra, are quantities associated with a particular sample member of the entire ensemble of earthquake ground motions. If a nondeterministic approach to structural analysis or design is used, the mean values and information about the variability of the ensemble response spectra are needed. The average response spectra and the corresponding standard deviations of the 25 synthesized earthquake samples are obtained by the Monte Carlo computation as described earlier and shown in Fig. 11. Note that these spectra represent only the elastic structural responses. For response analysis or design when inelastic behavior of structures is expected, the additional energy dissipation in the structural-foundation system should be taken into consideration.

It is understood that the vertical motion of an earthquake is generally less severe than, and is not of as much concern to structural designers as the horizontal motion. The accelerograms and response spectra of vertical motions may be taken as one-half to two-thirds the horizontal accelerograms and spectra shown in Figs. 9 and 10, respectively. This

TABLE I—SPECTRUM INTENSITY SCALING FACTORS

The following scaling factors are Spectrum Intensity Factors[23] ($SI_{0.2}$) normalized to 1 for an earthquake of Richter magnitude 6.3. Free-field horizontal ground motions and response spectra may be estimated for design purposes by multiplying the amplitude coordinates on Figs. 9, 10, and 11 by these scaling factors.

Richter Magnitude	Scaling Factor
5	0.6
5.7	0.8
6	0.9
6.3	1.0
6.7	1.1
8	1.5

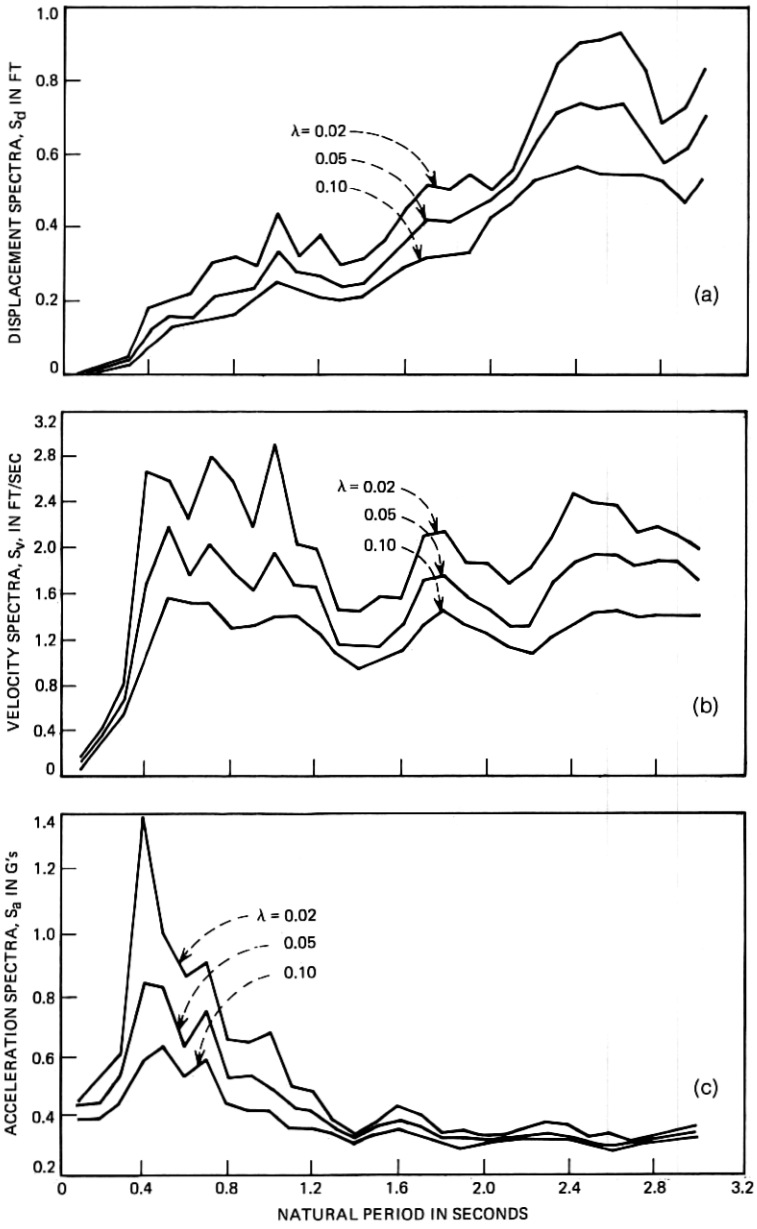

Fig. 10—Response spectra of earthquake accelerogram shown in Fig. 9.

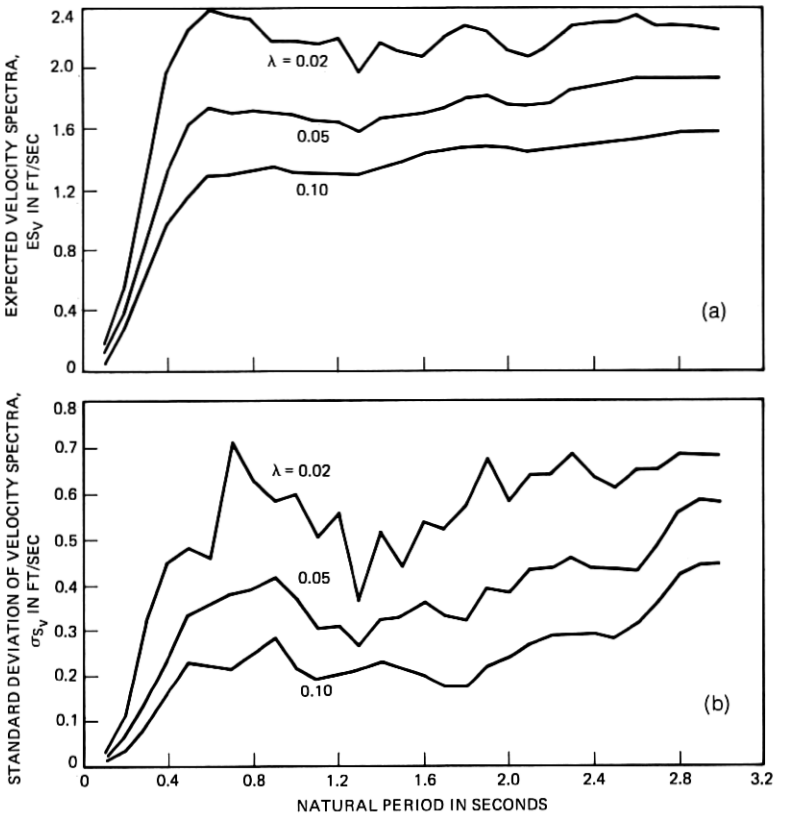

Fig. 11—Expected velocity spectra and standard deviation of an earthquake process with $M = 6.3$.

recommendation is made without the support of extensive theoretical analysis or data reduction as is done for the horizontal motion. However, it agrees with the limited data presently available, and it is consistent with the design practices adopted for other structures such as dams and nuclear power plants.[25]

3.3 *In-Building Motion Environments*

Telephone equipment installed within multistory buildings can generally be expected to encounter motion environments of greater intensity than equipment in single-story structures. Environments for the latter will be essentially free-field accelerograms, but multistory buildings amplify ground motions. It is not a trivial matter to specify

exactly how much amplification will take place, however, because the structural response of a building depends strongly on the properties of the structure and its founding soil. Soil properties affect not only the characteristics of the ground motions but also the fundamental frequency of the building. This in turn can drastically affect the way a building will vibrate and is generally referred to as soil-structure interaction.[26,27]

Typical fundamental frequencies for telephone buildings up to 20 stories tall and founded on various soils are also given in Fig. 8. If one examines building-frequency formulas found in the UBC, it will be noted that some nontelephone buildings have lower frequencies than those shown in Fig. 8. Telephone buildings are usually extremely well designed and constructed, and in spite of the massive equipment contained within them, their natural frequencies are generally higher than those of conventional office buildings.

It is important to understand that tall buildings, even the rigid ones constructed for telephone service, usually have fundamental frequencies that are below the dominant frequency contained in most earthquakes. This is fortunate because when the dominant frequency of an earthquake matches the fundamental frequency of a building, the acceleration responses of the structure can be much greater than in situations when these two frequencies do not match. This fact is illustrated in Fig. 12, which resulted from a study of the potential responses of a twenty-story building when subjected to earthquakes with various dominant frequencies.[27] It should be noted that the amplification of horizontal ground accelerations would clearly be highest when the earthquake's dominant frequency happens to match the structure's fundamental frequency and the building is founded on a stiff soil (V_s = 4000 ft/s). This hypothetical situation is unlikely to occur however; in fact, historical data that are shown on the frequency coordinate of Fig. 8 suggest that a frequency match should not be expected for telephone buildings that are over eight stories. A frequency match for buildings under eight stories will not result in amplifications that are as large as those given in Fig. 12. The estimated maximum ratios of in-building acceleration to horizontal ground motion that can be used for design purposes is shown in Fig. 13, which is a composite plot applicable to all telephone buildings up to 20 stories tall. These analytically-derived amplification factors may be regarded as upper-bound values that take into account the effects of the natural frequencies of the buildings, expected dominant frequencies of potential earthquakes, and all possible soil conditions on which buildings would conceivably be erected. Approximate in-building horizontal accelerograms can be artificially synthesized in a manner

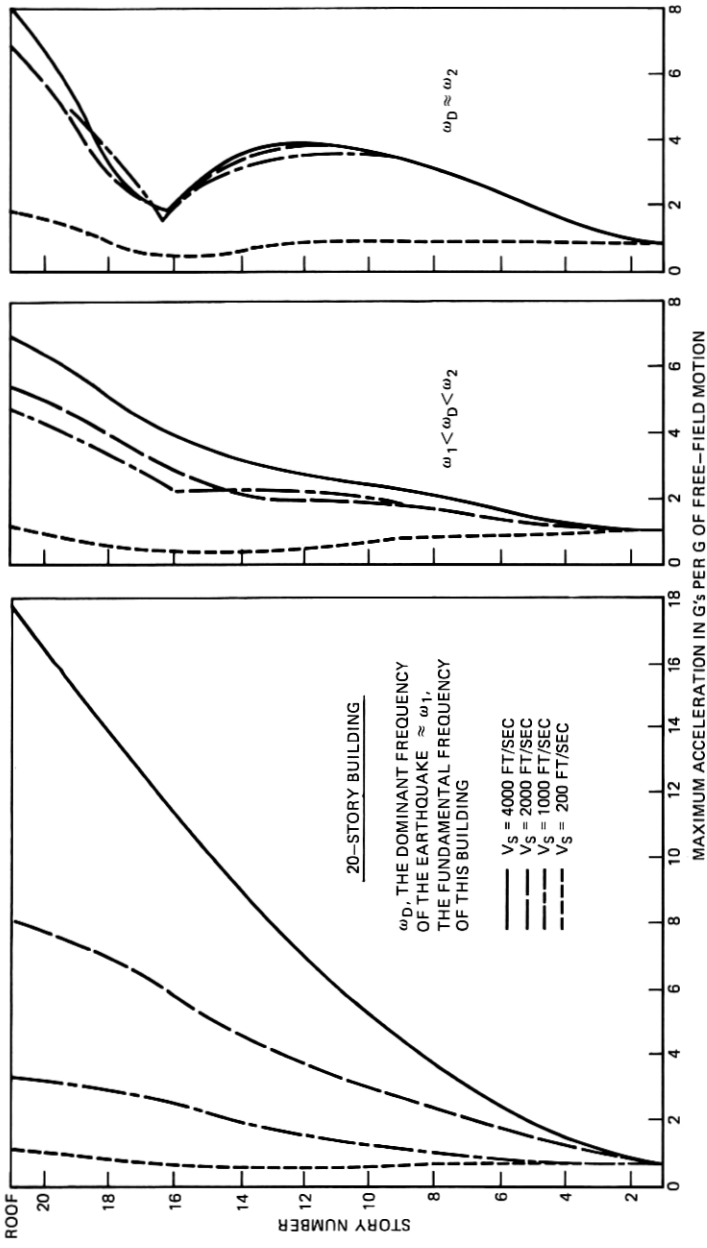

Fig. 12—Peak horizontal acceleration responses of 20-story buildings founded on various soils.

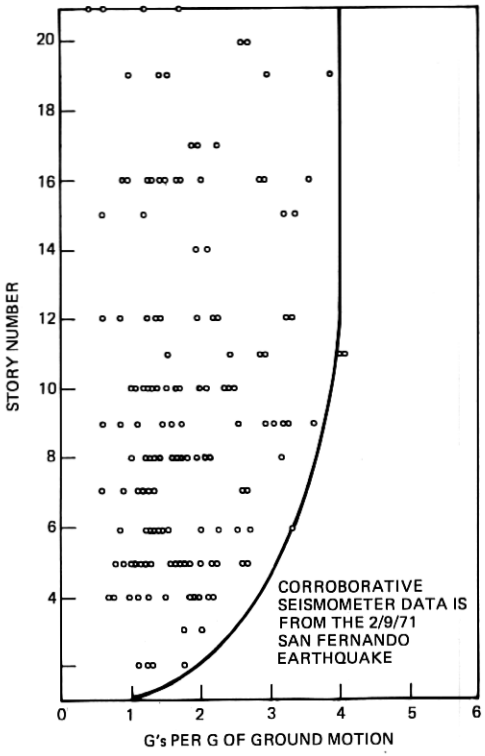

Fig. 13—Estimated practical upper bound for in-building horizontal accelerations during an earthquake.

similar to the generation of free-field motions, except that the value of $SI_{0.2}$ must be first multiplied by an amplification factor taken from Fig. 13. As an alternative to that procedure, the waveform shown in Fig. 9 and the corresponding response spectra in Figs. 10 and 11 may be multiplied by the appropriate scaling factor from Table I and also by the amplification factors given in Fig. 13. Note that these approximations are valid assuming there is no resonance between the building and the floor-mounted equipment.

IV. CONCLUDING REMARK

An extensive statistical analysis of seismicity data and earthquake motions has been made. Simple yet realistic stochastic models are used to describe the earthquake occurrence process and the random local

ground motion. Information useful for seismic design of the telephone system is generated according to the theory presented and through the use of an available strong earthquake catalog.

It should be pointed out that the main concern of this study is to provide information to assist in the physical design of earthquake-resistant structures by describing a realistic nationwide earthquake environment in meaningful engineering terms. The next step will be to establish appropriate structural design criteria. A simple approach for this would be to base such criteria on the most severe earthquake environment corresponding to the structure's expected service life (say 40 to 50 years) and knowledge of its stress, strain and deformation tolerance limits under dynamic loads. For important structures such as telephone central offices which house various sensitive and expensive electronic communications equipment, a more rigorous approach based on both the seismic risk and cost analyses is desirable. An optimal design strategy in terms of earthquake and structure parameters can be reached by achieving a balance in the total construction cost and the expected loss due to earthquake damage. The mathematical formulation and detailed analysis of such an optimum seismic design procedure are reported in a forthcoming paper in the B.S.T.J.[28]

Finally, it should be emphasized that the earthquake environments that are described are not intended, nor should they be construed, to be prophetic descriptions of future earthquakes. However, structures that are designed to adequately withstand these environments should consequently be expected to have a high probability of survival against earthquakes during their service life.

APPENDIX A

Approximate Solutions for the Peak Value Statistics of $x(t)$

Some approximate solutions can be obtained for the statistics of the peak amplitude of $x(t)$ in the following manner. Assume that for $\phi(t)$ in Fig. 2, the lengths of $t_1 - 0$ and $t_3 - t_2$ of the initial build-up and final decay are relatively short compared with the length $t_2 - t_1$ of the strong-motion phase of the accelerogram, and that the occurrence time $t^{(i)}$ of the extreme peak $z^{(i)}$ of a sample function $x^{(i)}(t)$ will always occur in the range $[t_1, t_2]$. These assumptions are justified from analyses of the behavior of structures under earthquake motion. Under these conditions and setting $\phi \equiv 1$, eq. (11) becomes

$$m_{|a|}(t) = \nu_n \exp\left(-\frac{a^2}{2\sigma_n^2}\right), \tag{12}$$

where $\nu_n = \sigma_{\dot{n}}/(\pi\sigma_n) = \omega_g/\pi$ is the expected number of zero crossings of the process $n(t)$ per unit time from both above and below. The problem is then reduced to a stationary one. Letting $t_0 = t_2 - t_1$ and using the logic that follows eq. (11) readily lead to the following approximate solutions:

$$F(z) = \exp\left(-\nu_n t_0 e^{-z^2/2\sigma_n^2}\right) \tag{13}$$

$$f(z) = \frac{\nu_n z t_0}{\sigma_n^2} \exp\left(-\frac{z^2}{2\sigma_n^2} - \nu_n t_0 e^{-z^2/2\sigma_n^2}\right), \tag{14}$$

$$\bar{z} \cong \left(A + \frac{\gamma}{A}\right)\sigma_n, \tag{15}$$

$$\overline{z^2} = (A^2 + 2\gamma\sigma_n^2), \tag{16}$$

and

$$\sigma_z^2 \cong \frac{\pi^2\sigma_n^2}{6A^2}, \tag{17}$$

where $A = (2 \ln \nu_n t_0)^{1/2}$ and γ is the Euler constant. If the ground acceleration is represented by a filtered white noise of constant power spectral density S, it can be shown that $\sigma_n = (S\pi/2\xi_g\omega_g^3)^{1/2}$ and that $\sigma_{\dot{n}} = \omega_g\sigma_n$, where ω_g and ξ_g are the natural frequency and damping constant of the simple ground filter. From eqs. (15) and (17) and the expression for σ_n, $\bar{z}$ and σ_z can be expressed in terms of t_0 and S.

APPENDIX B

Stationary Approximation for the Statistics of Response Process $u(t)$

The results for statistics of the response process $u(t)$ using the stationary approximation method are:

$$\sigma_u^2 = \frac{\pi\bar{S}_M B}{A_o(A_1 B - A_o A_3^2)}, \tag{18}$$

$$\sigma_{\dot{u}}^2 = \frac{\pi\bar{S}_M A_3}{A_1 B - A_o A_3^2}, \tag{19}$$

and

$$\nu_u = \frac{1}{\pi}\left(\frac{A_o A_3}{B}\right)^{\frac{1}{2}} \tag{20}$$

where $A_o = \omega_g^2\omega_o^2$, $A_1 = 2\omega_o\omega_g(\xi_o\omega_g + \xi_g\omega_o)$, $A_2 = \omega_o^2 + \omega_g^2 + 4\xi_o\xi_g\omega_o\omega_g$,

$A_3 = 2(\xi_o\omega_o + \xi_g\omega_g)$, $B = A_2A_3 = A_1$, and

$$\bar{S}_M = \frac{2\xi_g\omega_o^2\bar{z}_M^2A^2}{\pi(A^2 + \gamma)^2}. \tag{21}$$

The quantity $\bar{S}_M$ in eq. (21) is the expected uniform power spectral density of the white noise which will produce an earthquake process $x(t)$ of magnitude M with an expected peak ground acceleration $\bar{z}_M$ [see eq. (15)].

Now the response spectrum can be expressed in terms of $\bar{z}_M$. The relationship between $\bar{z}_M$ and M is shown in Fig. 3 based on the data from Housner.[23] The expected (pseudo-) velocity spectrum, defined as $S_v(\omega_o, \xi_o) = \omega_o \sup_t |u|$, is then given by

$$ES_v(\omega_o, \xi_o) = \omega_o K\sigma_n, \tag{22}$$

where $K = (2 \ln \nu_u t_o)^{1/2} + \gamma(2 \ln \nu_u t_o)^{-1/2}$. The standard deviation of the pseudovelocity spectrum, in analogy to eq. (17), is given by

$$\sigma_{s_v} = \omega_o\sigma \sup_t |u| = 1.28\omega_o\sigma_u/K. \tag{23}$$

REFERENCES

1. "Earthquake Engineering Research," Report to National Science Foundation, U. S. Dept. of Commerce Clearinghouse document, PB188636, 1969.
2. Fagel, L. W., Foss, J. W., and Liu, S. C., "The San Fernando Earthquake of February 9, 1971—Damage to Telephone Communications and Other Facilities," Unpublished work.
3. Uniform Building Code, Vol. I, International Conf. Building Officials, Pasadena, California, 1970.
4. DeCapua, N. J., Fagel, L. W., and Liu, S. C., "Earthquake Analysis of Telephone Building and ESS Equipment," Unpublished work.
5. "Earthquake History of the United States," Part I and Part II, U. S. Government Printing Office, 1961.
6. Algermissen, S. T., "Seismic Risk Studies in the United States," Proc. Fourth World Conference on Earthquake Engineering, Chile, *1* (January 1969), pp. 14–27.
7. Cox, D. R., and Lewis, P. A. W., *The Statistical Analysis of Series of Events*, London: Methuen, 1966.
8. Shlien, S., and Toksoj, M. N., "A Clustering Model for Earthquake Occurrences," Bull, Seism. Soc. Am., *60*, No. 6 (December 1970), pp. 1765–1787.
9. Vere-Jones, D., and Davies, R. B., "A Statistical Survey of Earthquakes in the Main Seismic Region of New Zealand, Part 2, Time Series Analysis," New Zealand J. Geol. Geophys, *9*, No. 3 (1966), pp. 251–284.
10. Knapoff, L., "The Statistics of Earthquakes in Southern California," Bull. Seismic Soc. Am. *54*, No. 6 (December 1964), pp. 1871–1873.
11. Isacks, B. L., Sykes, L. R., and Oliver, J., "Spatial and Temporal Clustering of Deep and Shallow Earthquakes in the Fiji-Tonga-Kernadec Region," Bull. Seism. Soc. Am. *57*, No. 5 (October 1967), pp. 935–958.
12. Ferraes, S. G., "Test of Poisson Process for Earthquakes in Mexico City," J. Geophys. Res. *72*, No. 14 (July 1967), pp. 3741–3742.
13. Page, R., "Aftershocks and Microaftershocks of the Great Alaskan Earthquake of 1964," Bull. Seism. Soc. Am., *58*, No. 3 (June 1968), pp. 1131–1168.

14. Aki, K., Hori, M., and Maturoto, H., "Aftershocks Observed at a Temporary Array Station on the Kenai Peninsula from May 19 to June 7, 1964," *The Prince William Sound, Alaskan Earthquake of 1964 and Aftershocks*, Vol. II, Parts B and C, 1969, pp. 131–156.
15. Kallberg, K. T., "Seismic Risk in Southern California," Research Rept. R69-31, Massachusetts Institute of Technology, Dept. of Civil Engineering, June 1969.
16. Vere-Jones, D., "Stochastic Models for Earthquake Occurrence," J. Royal Statist. Soc. B., *32*, No. 1 (1970) pp. 1–62.
17. Epstein, B., and Lomnitz, C., "A Model for the Occurrence of Large Earthquakes," *Nature, 211*, No. 5052 (August 1966), pp. 954–956.
18. Gumbel, E. J., "Statistical Theory of Extreme Values and Some Practical Applications," National Bureau of Standards, Appl. Math. Series 33, 1954.
19. Gutenberg, B. and Richter, C. F., "Earthquake Magnitude, Intensity, Energy and Acceleration," Bull. Seismological Soc. Amer. *46* (1956), pp. 105–143.
20. Liu, S. C., "Synthesis of Stochastic Representations of Ground Motions," B.S.T.J., *49*, No. 4 (April 1970) pp. 521–541.
21. Jennings, P. C., Housner, G. W., and Tsai, N. C., "Simulated Earthquake Motions," Tech. Rept. Earthquake Engineering Research Lab., California Inst. Tech., Pasadena, California, April 1968.
22. Liu, S. C., "On Multiplicative Processes," unpublished work.
23. Housner, G. W., "Intensity of Earthquake Ground Shocking Near the Causative Fault," Proc. Third World Conference on Earthquake Engineering, New Zealand, *1* (1965), pp. IV-94 to IV-111.
24. Liu, S. C., "Statistical Analysis and Stochastic Simulation of Ground-Motion Data," B.S.T.J., *47*, No. 10 (December 1968), pp. 2273–2298.
25. DiPol, C. V., "Seismic Design Criteria for Nuclear Power Plants," American Society of Civil Engineers National Meeting, New Orleans, La. February 1969, preprint paper no. 1791.
26. Liu, S. C., and Fagel, L. W., "Earthquake Interaction by Fast Fourier Transform," J. Eng. Mech. Div., ASCE, *97*, No. EM4 (August 1971), pp. 1223–1237.
27. Fagel, L. W., and Liu, S. C., "Earthquake Interaction for Multistory Buildings," J. Eng. Mech. Div., ASCE, *98*, No. EM4 (August 1972), pp. 929–945.
28. Liu, S. C., and Neghabat, F., "A Cost Optimization Model for Seismic Design of Structures," B.S.T.J., *51*, No. 10 (December 1972).